Supplementary Material for "Molecular Dynamics Simulations of DNA/PEI Complexes: Effect of PEI Branching and Protonation State"

Chongbo Sun, Tian Tang,* Hasan Uludağ, and Javier E. Cuervo

S1 Details about developing the force field for PEI

The force field for PEI were developed based on the CHARMM General Force Field (CGenFF).[1] The force field for the building blocks of PEI are available in CGenFF, which are "RESI EAMM, $CH_3-CH_2-NH_3$", "RESI DMAM, $CH_3-NH-CH_3$", and "RESI TMAM, $N-(CH_3)_3$", corresponding to the primary, secondary and tertiary amines, respectively. Based on these three residues all van der Walls parameters, most bonded parameters, and partial charges for each atom were determined. The remaining angle and torsion parameters were adopted from existing parameters for analogous atom groups in CGenFF. It has been argued, in the CGenFF paper,[1] that this methodology can be advantageous over bonded parameters parameterized from quantum mechanics calculations as the existing parameters have been further tuned and validated against experiments after the initial quantum mechanics calculations.

*To whom correspondence should be addressed

S2 Complex formation using CHARMM force field (this work) *VS.* using AMBER force field (Ref. 2)

To examine how the complex formation can be affected by using different force fields, we made a comparison to Ref. 2, where AMBER force field was used, by performing a simulation of 'System 50%-PEI(20)' defined in Ref. 2 with the same simulation procedure. Very close results were obtained, demonstrating the similarity of these two force fields in describing the DNA/PEI systems.

The simulation parameters reported in Ref. 2 were adopted as much as possible in our simulation:

1. A 20 monomers purely linear PEI (see definition of "purely linear" in the main texts) with 10 monomers (index 2, 4, 6, 7, 12, 13, 14, 16, 17 and 20) protonated;
2. 27 Na+, 15 Cl- counterions added in the water box to neutralize the system;
3. 50 Å initial separation between the DNA and PEI centers of mass;
4. SHAKE algorithm, 2 fs time step;
5. 10 Å cutoff for van der Waals and direct electrostatic calculation;
6. Particle mesh Ewald method;
7. 20 ps of heating to 300K after the minimization;
8. 1.2 ns NPT simulation with restraints on DNA and PEI after heating.

The differences between the two simulations exist in the following aspects:

1. Force field: CHARMM (Our simulation) vs. Amber (Ref. 1);
2. Initial configurations of PEI and initial relative position of DNA and PEI;
3. Water box size: $84 \times 93 \times 92$ Å^3 (our simulation) vs. $95 \times 100 \times 80$ Å^3 (Ref. 2);

4. Simulation time: we used a much longer simulation time (40 ns and 60 ns) since it appears that it took longer for our system to equilibrate.

S2.1 Results

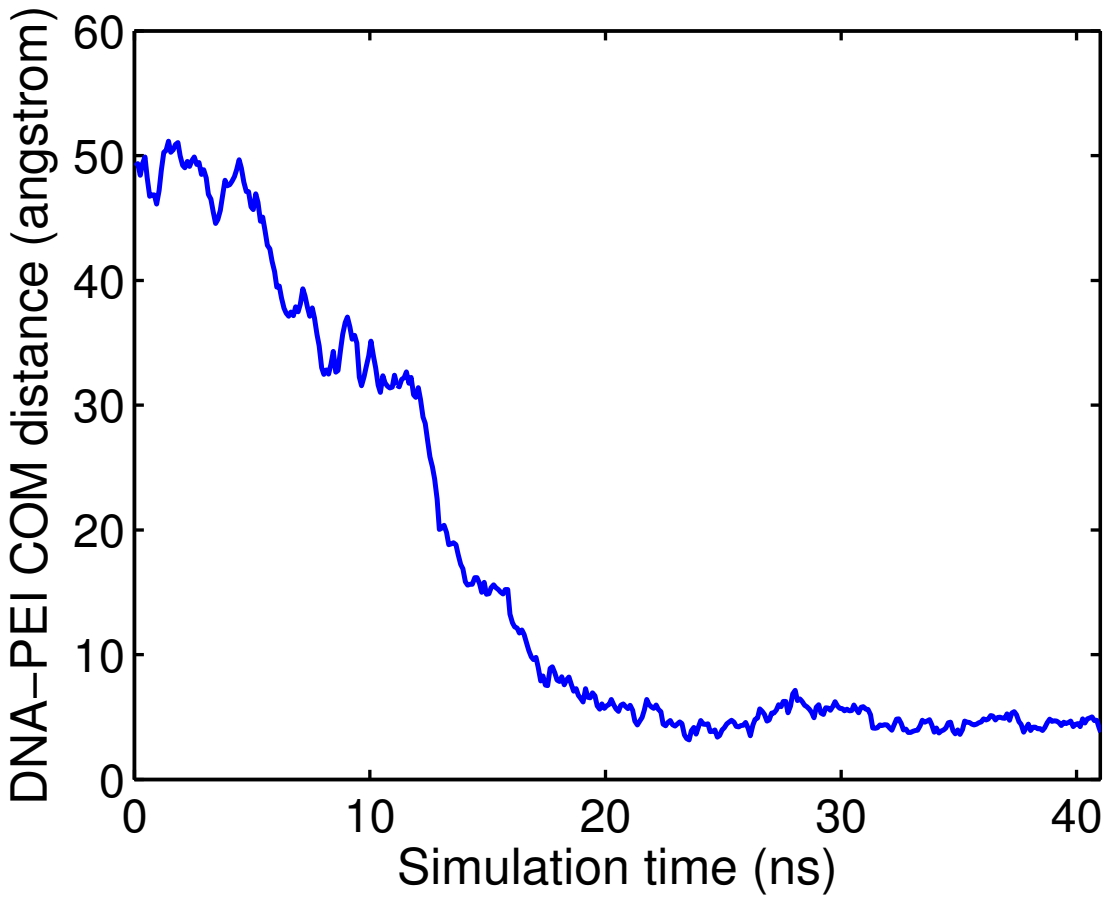

Figure S1: Center of mass distance between the DNA and the PEI as a function of simulation time. Time is zeroed at the moment when the restraints were removed from the DNA and the PEI.

Figure S1 plots the center of mass (COM) distance between the DNA and the PEI as a function of simulation time. The COM distance fluctuates around a constant for several ns at the beginning of the simulation and again at about 8-12 ns, but overall the COM distance decreases as the PEI approaches the DNA. The COM distance becomes stable at about 20 ns of the simulation when the complex has been formed with a significant part of the PEI in close contact with the DNA. The same characteristics was found in Ref. 2 (Shown in Figure S2), however the rates of the complex

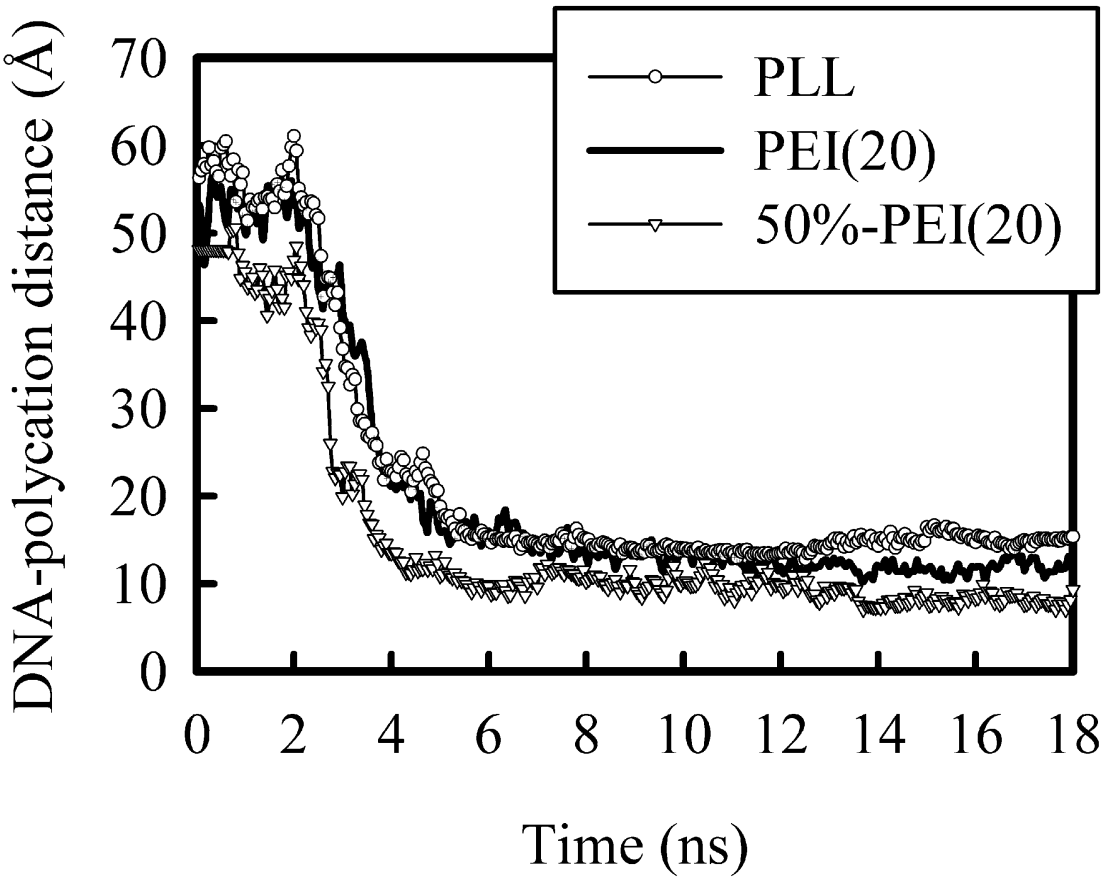

FIGURE 1 Plot of the distance between the centers of mass of DNA and the polycation chains as a function of simulation time for the first three systems, PEI(20), PLL(20), and 50%-PEI(20). Time zero corresponds to the moment when restraints on the chains were removed.

Figure S2: Figure 1 from Ref. 2.[3]

formation in the two simulations are different. In our simulation the COM distance takes about 20 ns to stabilize, while in Ziebarth's simulation it only took about 5 ns. This could be due to the different force field used, but more probably, it may be due to the difference in the initial position of the PEI relative to the DNA and hence the positions of the image molecules (from periodic boundary condition).

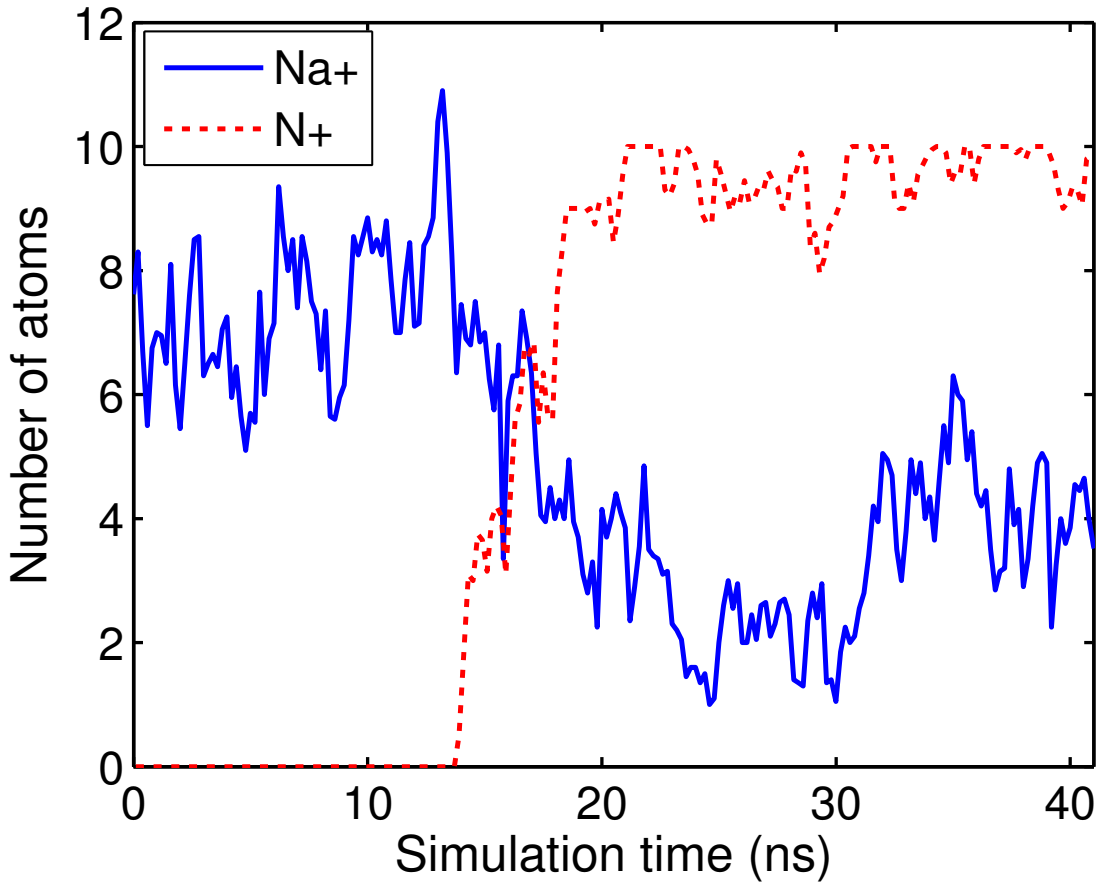

Figure S3: The number of Na+ ions and protonated amine nitrogens within 10 Å of any C1' DNA atom as a function of time.

Figure S3 plots the number of Na+ ions and protonated amine nitrogens within 10 Å of any C1' DNA atom as a function of time. As the PEI approaches the DNA, the number of Na+ decreases from a value of about 7 to about 3, indicating the release of Na+ around DNA is due to its association with the PEI. This curve was not plotted for the same system (DNA and a purely-linear 50% protonated PEI with 20 amine groups) in Ref. 2, however, the same phenomenon was found for system I (DNA and a 100% protonated PEI with 20 amine groups) in FIGURE 3 of Ref. 2 (Shown in Figure S4).

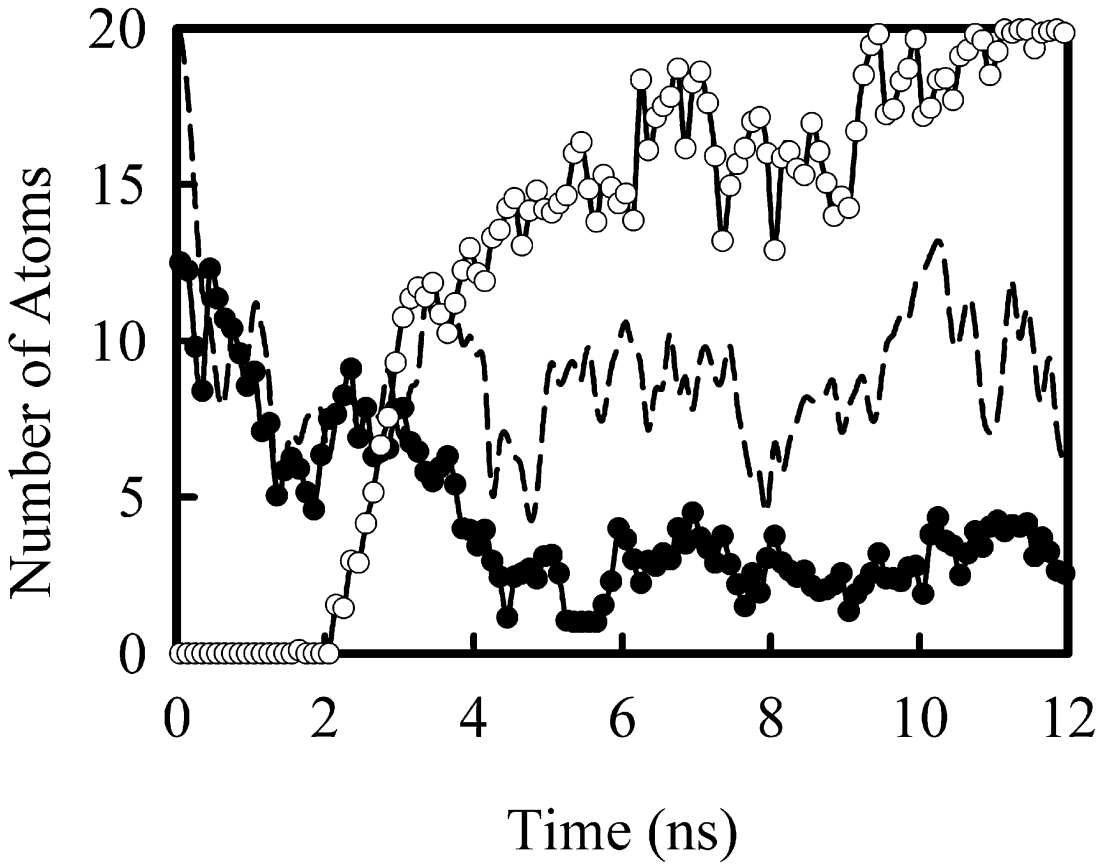

FIGURE 3 Plot of the number of Na^+ ions (*solid circles*) and protonated amine nitrogens (*open circles*) for system I (PEI(20)) within 10 Å of any C1′ DNA atom as a function of time for system I (PEI(20)). The dashed line shows the number of Na^+ ions for system VI as a reference. The number of Na^+ ion around DNA helix is reduced as PEI chain approaches the DNA helix.

Figure S4: Figure 3 from Ref. 2.[3]

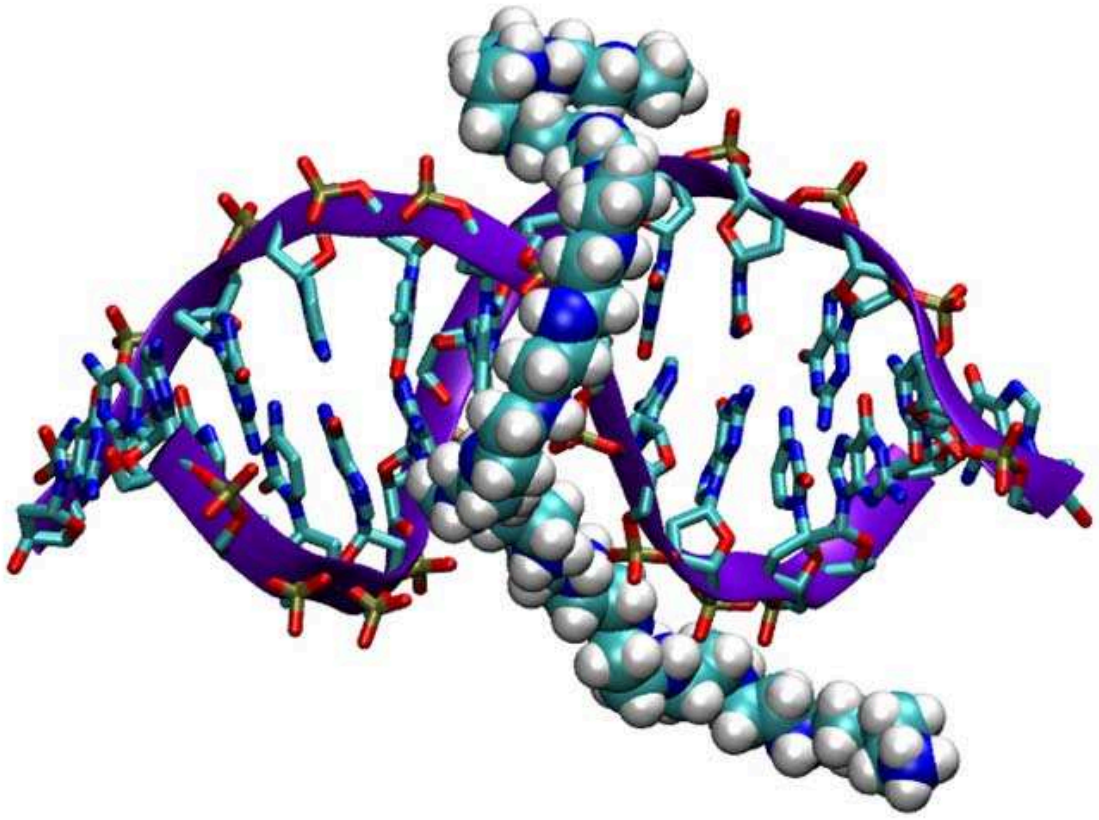

Figure S5: A snapshot of the complex at the final stage of MD.

Figure S5 is a snapshot of the complex at the final stage of the molecular dynamics (MD) simulation. The PEI is mainly in contact with only one strand of the DNA with a significant section of the PEI comply to the backbone of one DNA strand. The snapshot looks similar to the snapshot for the same system shown in FIGURE 6(f) of Ref. 2 (not shown here).

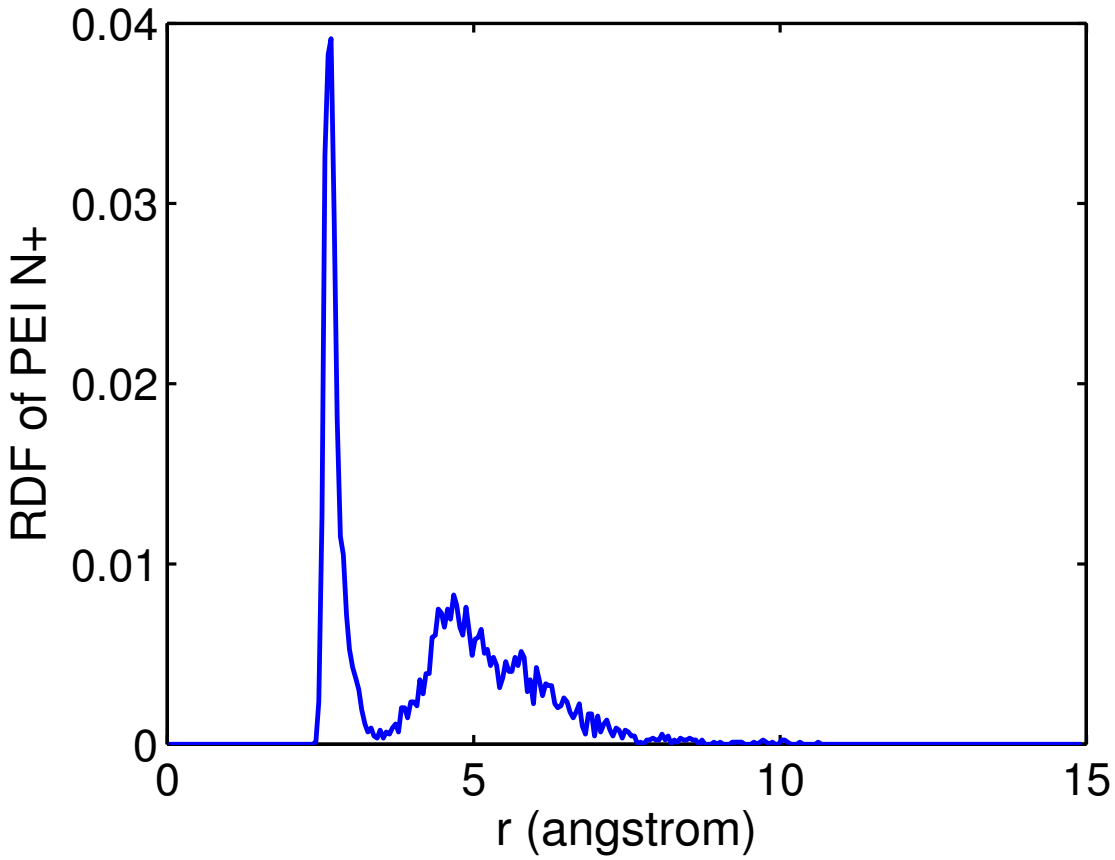

Figure S6: Radial distribution functions (RDF) of Nitrogen atoms in protonated amine groups around the O1P and O2P DNA atoms.

Figure S6 is the radial distribution functions (RDF) of Nitrogen atoms in protonated amine groups around the O1P and O2P DNA atoms, where distance step 0.05 Å was used in generating the figure. The RDF curve has two peaks, one at about 3 Å and the other one at about 5 Å. The first peak corresponds to direct contact between the amine groups and the DNA O1P, O2P atoms, the second peak corresponds to secondary interaction such as water-mediated hydrogen bonding. The RDF curve resembles that in FIGURE 7 of Ref. 2 (Shown in Figure S7).

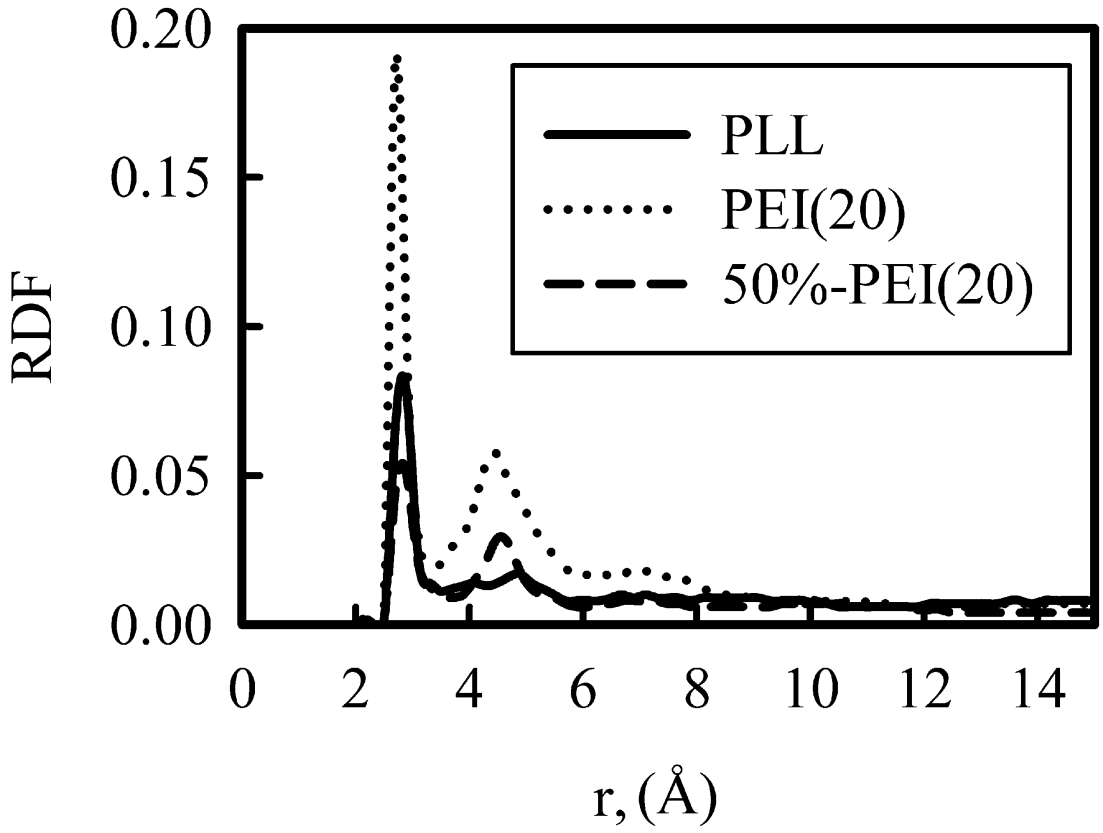

FIGURE 7 Radial distribution functions of polycation amine groups shown in figure legends around the O1P and O2P DNA atoms. In the case of the 50%-PEI(20) simulation, only charged amine groups are included.

Figure S7: Figure 7 from Ref. 2.[3]

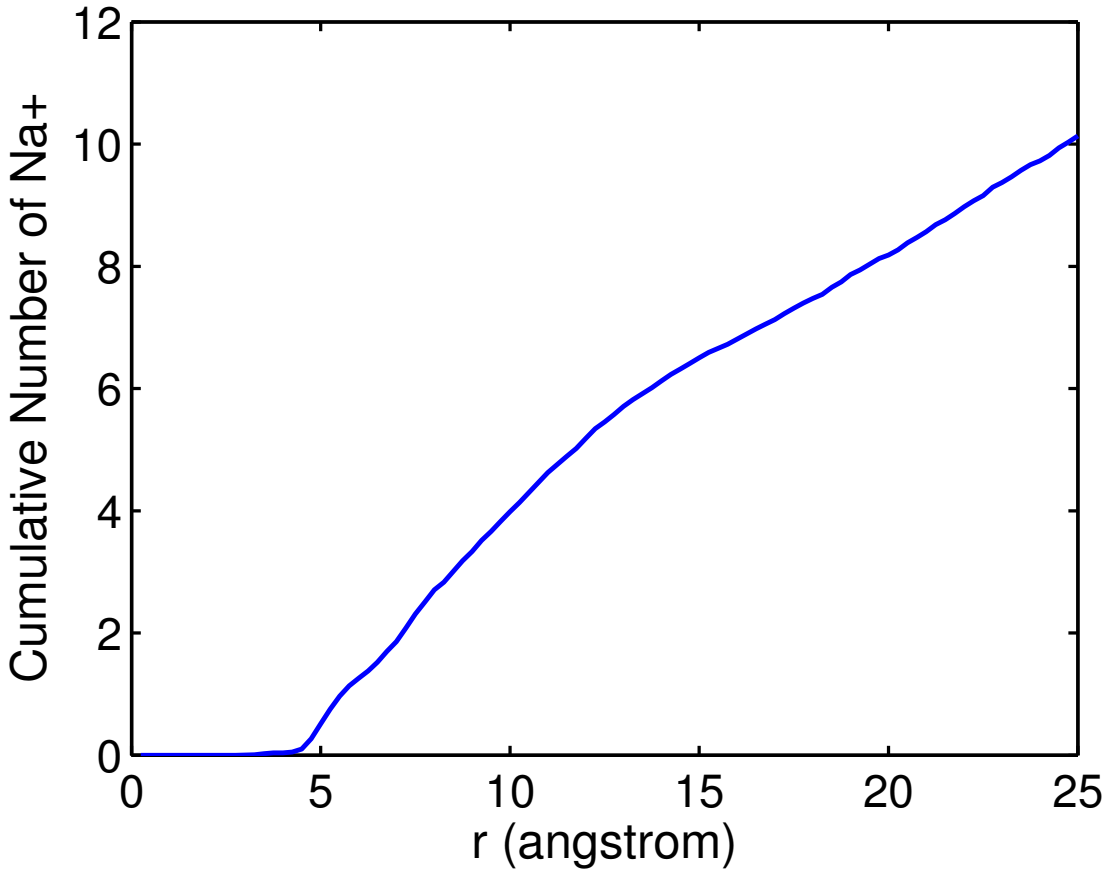

Figure S8: Cumulative number of sodium ions as a function of the distance from any C1' DNA atom.

Figure S8 shows the average cumulative number of sodium ions as a function of the distance from any C1' DNA atom during the last 6 ns of the simulation. The closet Na+ exists at about 5 Å from the C1' atoms. From 5 Å to 25 Å, the number of Na+ around the DNA gradually increases and approximately 10 Na+ are within 25 Å. The curve is very similar to the curve for 50%-PEI(20) in FIGURE 8 of Ref. 2 (Shown as dotted line in Figure S9).

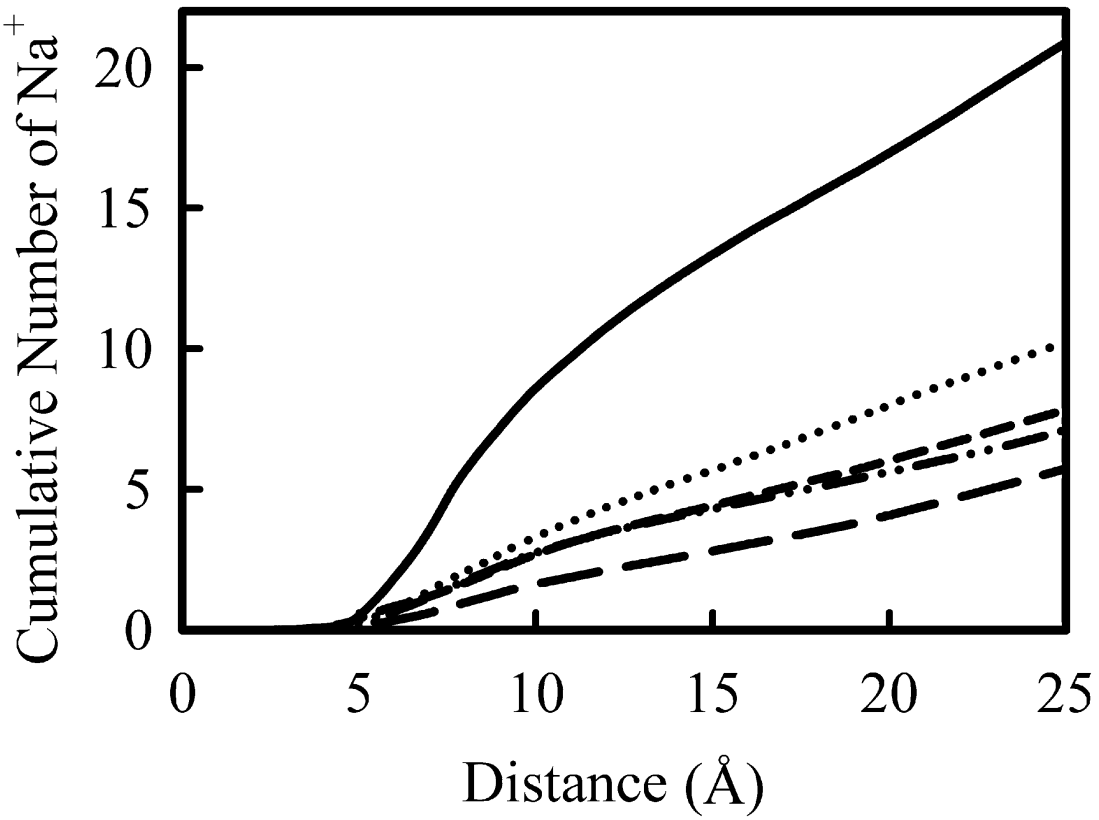

FIGURE 8 Cumulative number of sodium ions as a function of the distance from any C1′ DNA atom for each simulation. From the top line down, the Na^+ (*solid line*), 50%-PEI(20) (*dotted line*), PEI(20) (*short dashes*), PLL (*dots-dashes*), and 50%-PEI(40) (*long dashes*) systems are shown.

Figure S9: Figure 8 from Ref. 2.[3]

S3 Torsional parameters validation

In order to verify the correctness of the torsional parameters used for PEIs in the MD simulations, we have calculated the torsional potential energy surface (PES) as a function of certain representative dihedral angles at *ab initio* and molecular mechanics (MM) levels. Five compound models were used to calculated the PES: neutral N-Ethylethylenediamine (2-MI), secondary amine protonated N-Ethylethylenediamine (2-MI-P-A), primary amine protonated N-Ethylethylenediamine (2-MI-P-B), neutral branched trimethylimine (3-TMI) and primary amine protonated branched trimethylimine (3-TMI-P). The structure and atom type information of these five models is shown in Figure S10. In conjunction, the five models encompass all 13 possible combinations of non-hydrogen atom types in a dihedral term for the PEIs studied in this work. The studied dihedrals are summarize in Table S1. The *ab initio* quantum mechanical (QM) calculations were carried out using Gaussian 09[4] at MP2/6-31+G* level. The MM calculations were performed using package CHARMM 33b2[5] with our devised force field for PEI. For each dihedrals, 25 dihedral angles were calculated from -180° to 180° at an interval of 15°.

Figures S11 to S23 show the comparison of the PES calculated using QM and MM for the 13 dihedrals, respectively. A good agreement is observed in between the QM-PES and the MM-PES. In particular the overall shape, location of the maxima and minima and most of the relative energies of the QM model are reproduced by the MM calculation. For some dihedrals (e.g., NZ0-CX0-CX2-NZ2 shown in Figure S20), evident discrepancies exist, however the overall behavior is reproduced. The results obtained support the notion that the parameters used in the MD simulation make a model that is a good description of the intra-molecular interactions in the PEIs.

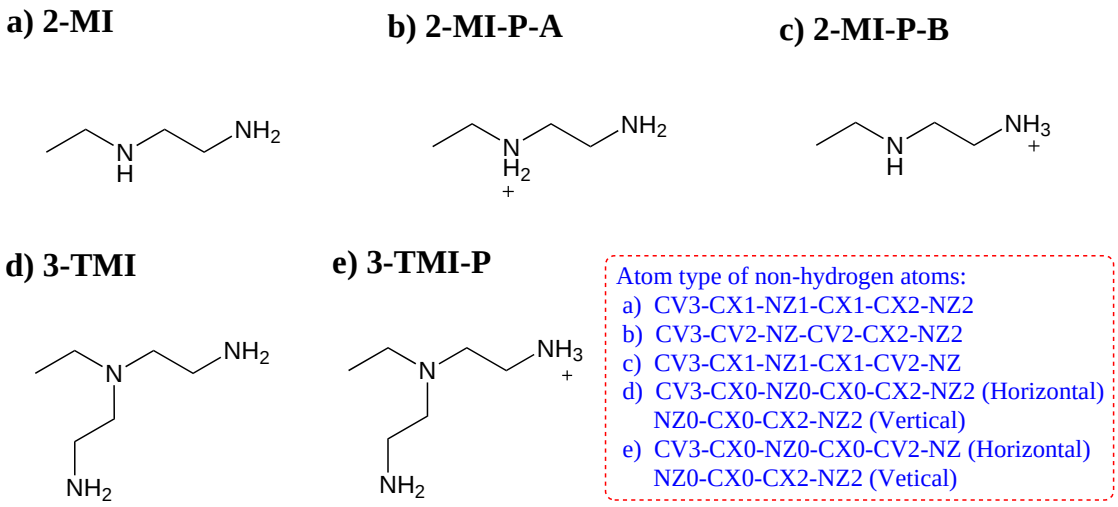

Figure S10: Molecular structures of the five compound models. (a) neutral N-Ethylethylenediamine (2-MI), (b) secondary amine protonated N-Ethylethylenediamine (2-MI-P-A), (c) primary amine protonated N-Ethylethylenediamine (2-MI-P-B), (d) neutral branched trimethylimine (3-TMI), (e) primary amine protonated branched trimethylimine (3-TMI-P). Atom types of the atoms in each compound are specified in the red dashed square: for (a), (b), (c), the list corresponds to the atom types of the non-hydrogen atoms in the chain from left to right; for (c), (d), the first list corresponds the atom types of the non-hydrogen atoms in the horizontal chain from left to right, and the second list corresponds to the non-hydrogen atoms in the vertical branch from top to bottom.

Table S1: The 13 dihedrals calculated

Dihedral	Model compound	QM/MM profiles
CV3-CX1-NZ1-CX1	2-MI	Figure S11
CX1-NZ1-CX1-CX2	2-MI	Figure S12
NZ1-CX1-CX2-NZ2	2-MI	Figure S13
CV3-CV2-NZ-CV2	2-MI-A	Figure S14
CV2-NZ-CV2-CX2	2-MI-A	Figure S15
NZ-CV2-CX2-NZ2	2-MI-A	Figure S16
CX1-NZ1-CX1-CV2	2-MI-B	Figure S17
NZ1-CX1-CV2-NZ	2-MI-B	Figure S18
CV3-CX0-NZ0-CX0	3-TMI	Figure S19
NZ0-CX0-CX2-NZ2	3-TMI	Figure S20
CX0-NZ0-CX0-CV2	3-TMI-P	Figure S21
NZ0-CX0-CV2-NZ	3-TMI-P	Figure S22
CX0-NZ0-CX0-CX2	3-TMI-P	Figure S23

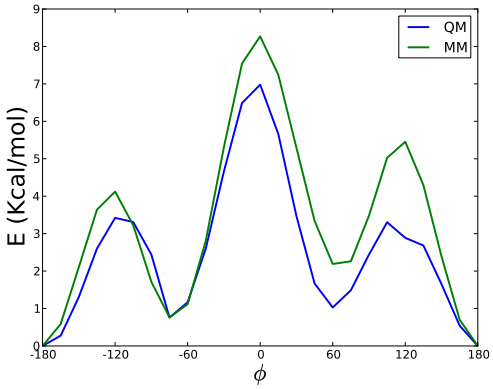

Figure S11: Potential energy profiles of dihedral CV3-CX1-NZ1-CX1 calculated using QM and MM.

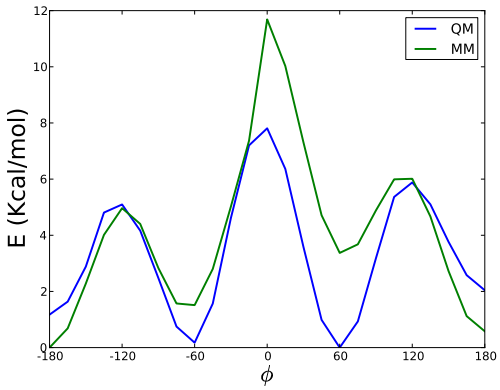

Figure S12: Potential energy profiles of dihedral CX1-NZ1-CX1-CX2 calculated using QM and MM.

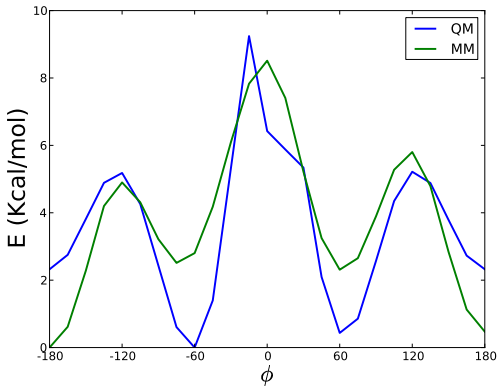

Figure S13: Potential energy profiles of dihedral NZ1-CX1-CX2-NZ2 calculated using QM and MM.

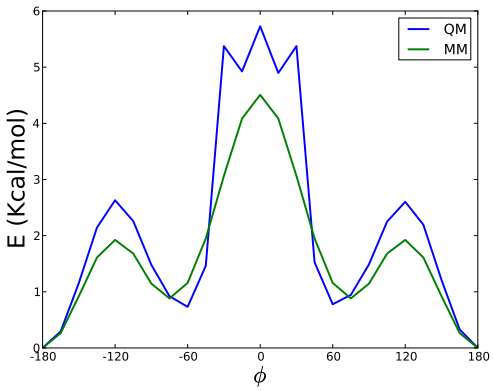

Figure S14: Potential energy profiles of dihedral CV3-CV2-NZ-CV2 calculated using QM and MM.

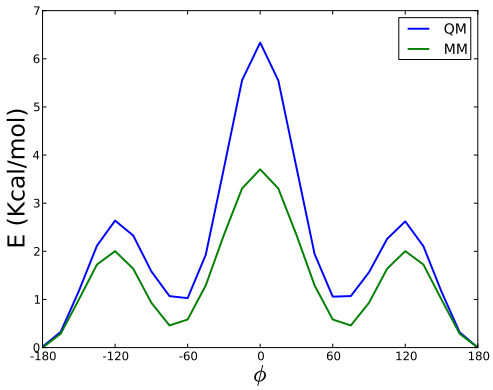

Figure S15: Potential energy profiles of dihedral CV2-NZ-CV2-CX2 calculated using QM and MM.

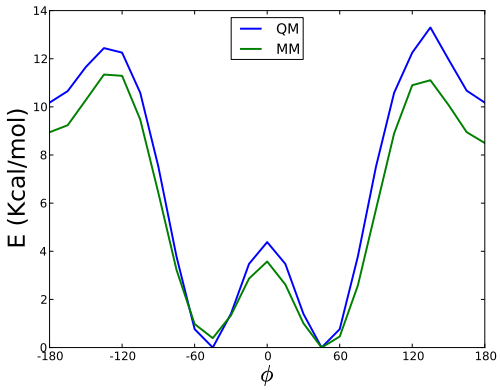

Figure S16: Potential energy profiles of dihedral NZ-CV2-CX2-NZ2 calculated using QM and MM.

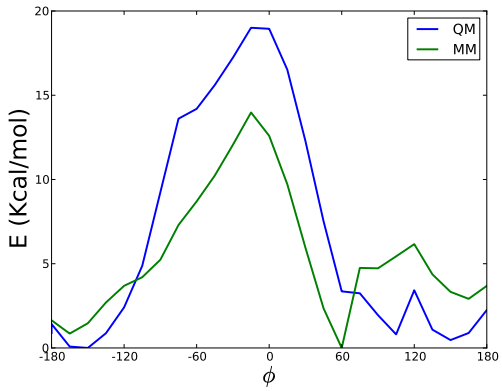

Figure S17: Potential energy profiles of dihedral CX1-NZ1-CX1-CV2 calculated using QM and MM.

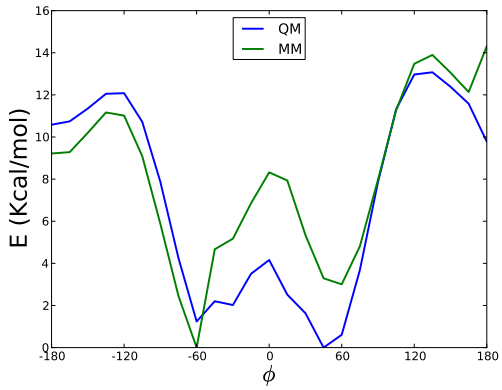

Figure S18: Potential energy profiles of dihedral NZ1-CX1-CV2-NZ calculated using QM and MM.

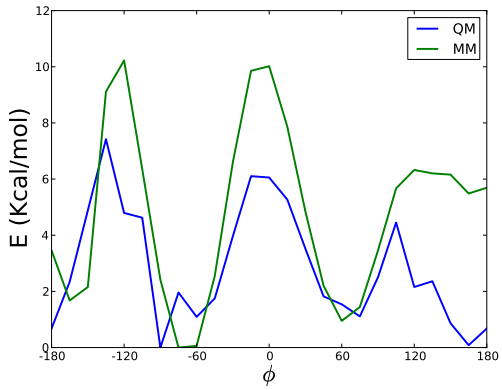

Figure S19: Potential energy profiles of dihedral CV3-CX0-NZ0-CX0 calculated using QM and MM.

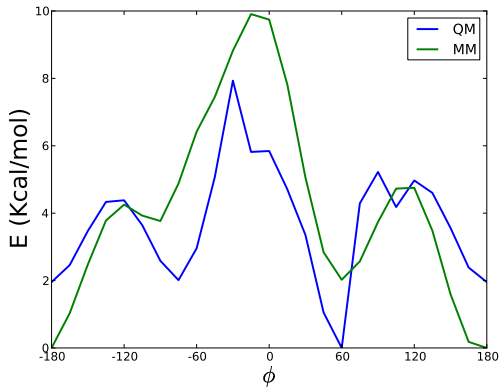

Figure S20: Potential energy profiles of dihedral NZ0-CX0-CX2-NZ2 calculated using QM and MM.

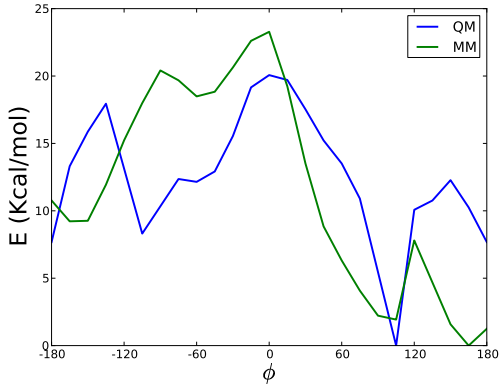

Figure S21: Potential energy profiles of dihedral CX0-NZ0-CX0-CV2 calculated using QM and MM.

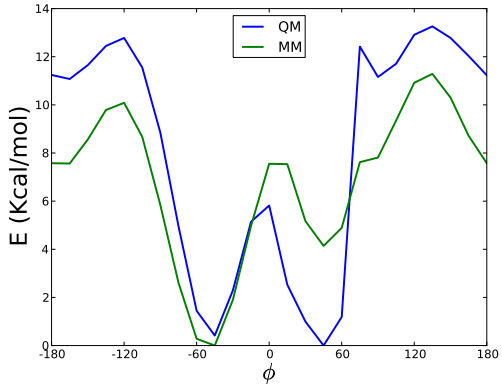

Figure S22: Potential energy profiles of dihedral NZ0-CX0-CV2-NZ calculated using QM and MM.

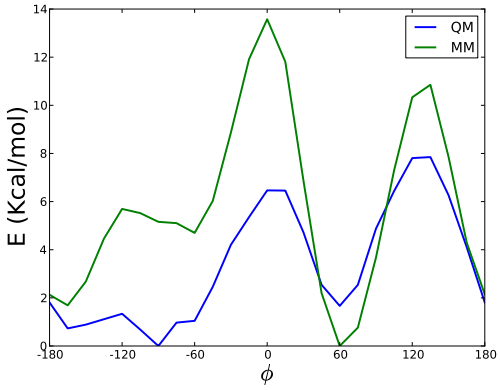

Figure S23: Potential energy profiles of dihedral CX0-NZ0-CX0-CX2 calculated using QM and MM.

S4 The sensitivity of DNA/PEI binding pattern to the torsional parameters of the PEIs

We have also examined how sensitive our results are to variations in the torsional parameters. To do this, we replaced our 13 dihedral parameters completely with that used in Dong's MD simulations of PEI[6] and repeated two of the eight MD simulations for DNA/PEI complex formation (23%-PL and 46%-HB). The torsional parameters for PEI used in Dong's simulation were obtained by "fitting an energy profile from a density functional calculation of for dimethylethylenediamine (DMEDA) into the dihedral angle torsion functional form",[6] and the simulations yielded good results in comparison with experimental data. Table S2 summaries the torsional parameters used in our work and in Ref. 6, where the torsional energy function is in the form of $E_{\text{torsion}} = k_\phi(1 + \cos(n\phi - \delta))$.

Figures S24 and S25 show the RDF and cumulative number of the PEI nitrogens around the DNA backbone oxygens based on the last 20 ns trajectory of the simulations for the 23%-PL system and the 46%-HB system, respectively. It can be observed from Figures S24 and S25 that, using a different set of torsional parameters which were derived from density function calculations and have been validated against experimental data, very similar results to our previous ones were obtained. Specially, the discrepancies associated with the two sets of torsional parameters in Fig-

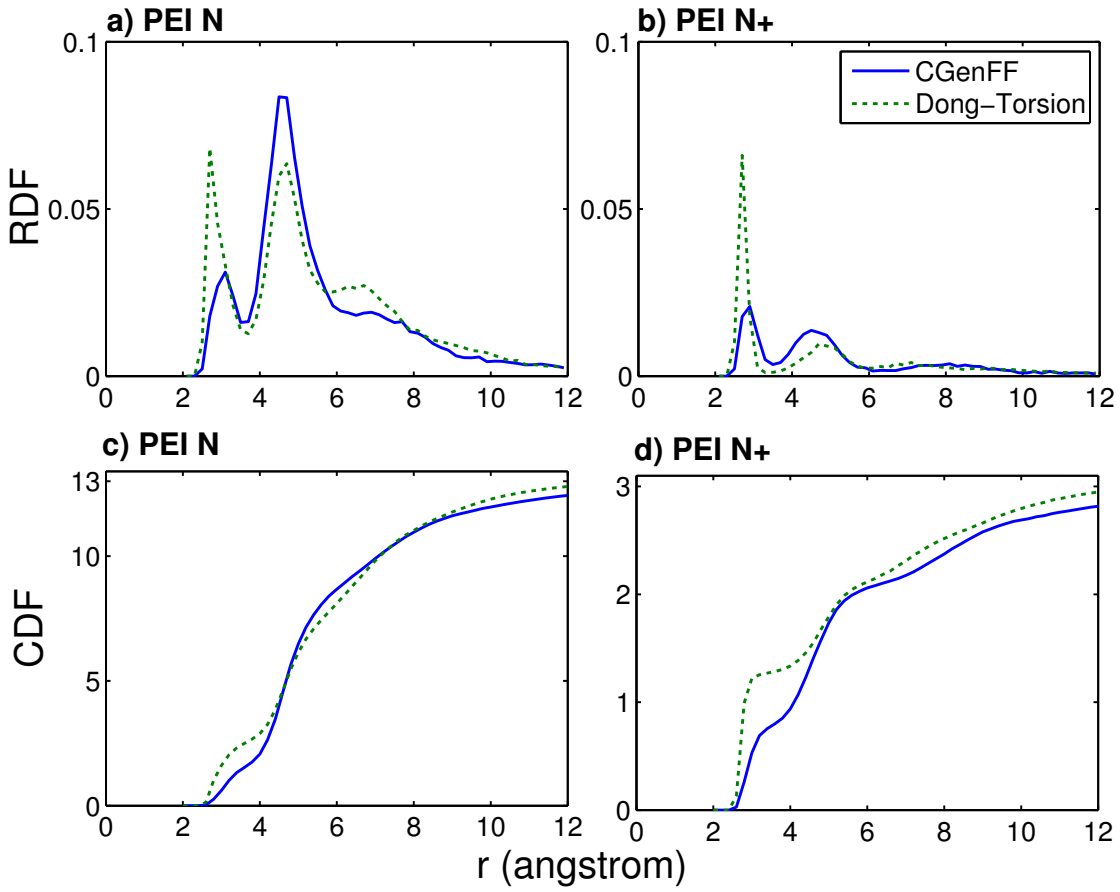

Figure S24: Radial distribution function (RDF) and cumulative number (CDF) of the PEI nitrogens around the DNA backbone oxygens based on the last 20 ns trajectory of the simulations for 23%-PL system. (a) RDF of all PEI nitrogens, (b) RDF of protonated PEI nitrogens, (c) CDF of all PEI nitrogens, (d) CDF of protonated PEI nitrogens.

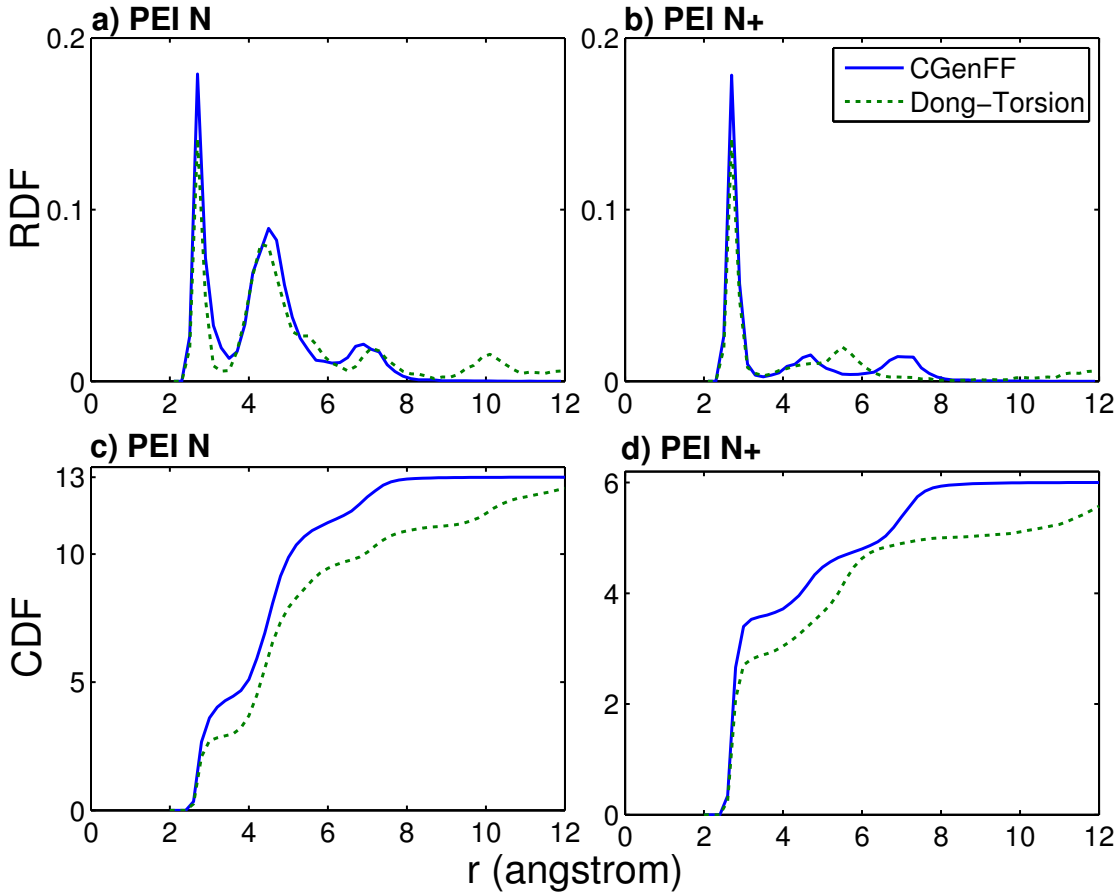

Figure S25: Radial distribution function (RDF) and cumulative number (CDF) of the PEI nitrogens around the DNA backbone oxygens based on the last 20 ns trajectory of the simulations for 46%-HB system. (a) RDF of all PEI nitrogens, (b) RDF of protonated PEI nitrogens, (c) CDF of all PEI nitrogens, (d) CDF of protonated PEI nitrogens.

Table S2: Torsional parameters of the 13 dihedrals. k_ϕ in kcal/mol, and δ in degree.

Dihedral	CGeenFF			Dong's work[6]		
	k_ϕ	n	δ	k_ϕ	n	δ
CV3-CX1-NZ1-CX1	1.26	3	0	1.0	3	0
CX1-NZ1-CX1-CX2	1.26	3	0	1.0	3	0
NZ1-CX1-CX2-NZ2	0.15	3	0	0.6	3	0
CV3-CV2-NZ-CV2	0.10	3	0	1.0	3	0
CV2-NZ-CV2-CX2	0.10	3	0	1.0	3	0
NZ-CV2-CX2-NZ2	0.15	3	0	0.6	3	0
CX1-NZ1-CX1-CV2	1.26	3	0	1.0	3	0
NZ1-CX1-CV2-NZ	0.15	3	0	0.6	3	0
CV3-CX0-NZ0-CX0	1.26	3	0	1.0	3	0
NZ0-CX0-CX2-NZ2	0.15	3	0	0.6	3	0
CX0-NZ0-CX0-CV2	1.26	3	0	1.0	3	0
NZ0-CX0-CV2-NZ	0.15	3	0	0.6	3	0
CX0-NZ0-CX0-CX2	1.26	3	0	1.0	3	0

ures S24 and S25 are comparable with the discrepancies among different simulation time windows using a single set of parameters as shown in Section S5 of this document (Figures S26 to S33). For example, the discrepancies in Figure S24(a) are comparable with the discrepancies in Figure S26 among different simulation windows. None of the new results obtained using Dong's torsional parameters changes the conclusions we made in the manuscript.

Based on the calculations in Sections S3 and S4, we believe that, for the focus of our study here which is the binding of DNA with PEIs, the force field we used is quantitatively meaningful. The force field for PEI might need to be further calibrated and validated if the objective is to study the conformation of PEIs in solution or crystal PEIs. However to study its binding to DNA, using the CGenFF principle to generate the force field parameters is a valid approach.

S5 Radial distribution function (RDF) and cumulative number curves within different time windows in the simulations

Figure S26 and Figure S27 are respectively the RDF plots for all PEI nitrogens and for the protonated PEI nitrogens around the DNA backbone oxygens in the 23% systems. Figure S28 and Figure S29 are the same RDF plots for the 46% systems. Figures S30 to S33 are the corresponding cumulative number plots for 23% systems and 46% systems, respectively. These RDF and cumulative number plots were generated based on trajectories within different time windows in the simulations.

Figures S26, S27, S30 and S31 show that even after 49 ns of simulation, the curves are still evolving with time, and the order of the curves corresponding to different PEI structures do not maintain the same at all time. This indicates that the complexes formed in the 23% systems are not stable, which is consistent with the fact that the majority of the nitrogens bind to DNA through indirect interactions. Compared with the 23% systems, the RDF and cumulative number curves for the 46% systems in Figures S28, S29, S32 and S33 demonstrate more stability (i.e., less variations among different simulation windows). Moreover, the curves corresponding to different PEI structures are closer to one another compared with the 23% systems. In fact, after 40 ns of simulations, these curves essentially overlap with one another. This indicates that at the protonation ration of 46%, the degree of branching has vanishingly small effect on the binding.

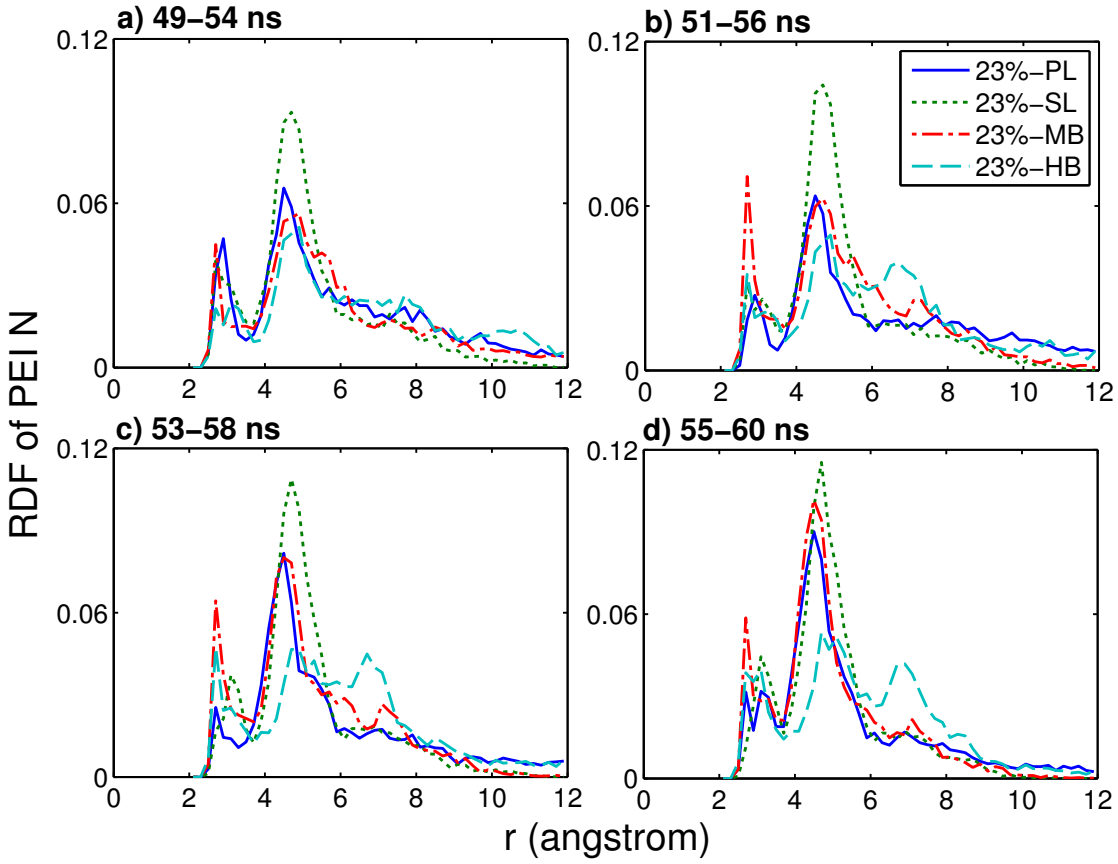

Figure S26: Radial distribution functions of all PEI nitrogens around the DNA backbone oxygens for the 23% systems, plotted for different simulation time windows. (a) 49–54 ns, (b) 51–56 ns, (c) 53–58 ns, (d) 55–60 ns.

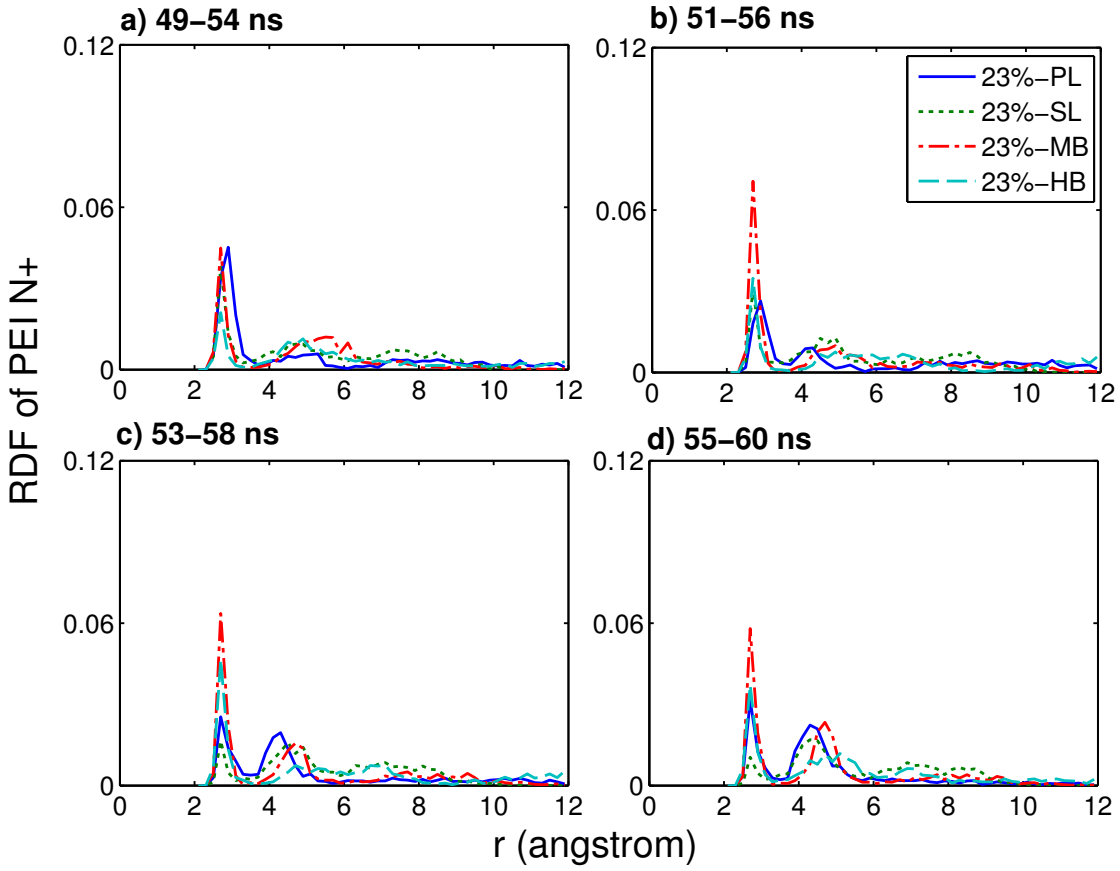

Figure S27: Radial distribution functions of the PEI protonated nitrogens around the DNA backbone oxygens for the 23% systems, plotted for different simulation time windows. (a) 49–54 ns, (b) 51–56 ns, (c) 53–58 ns, (d) 55–60 ns.

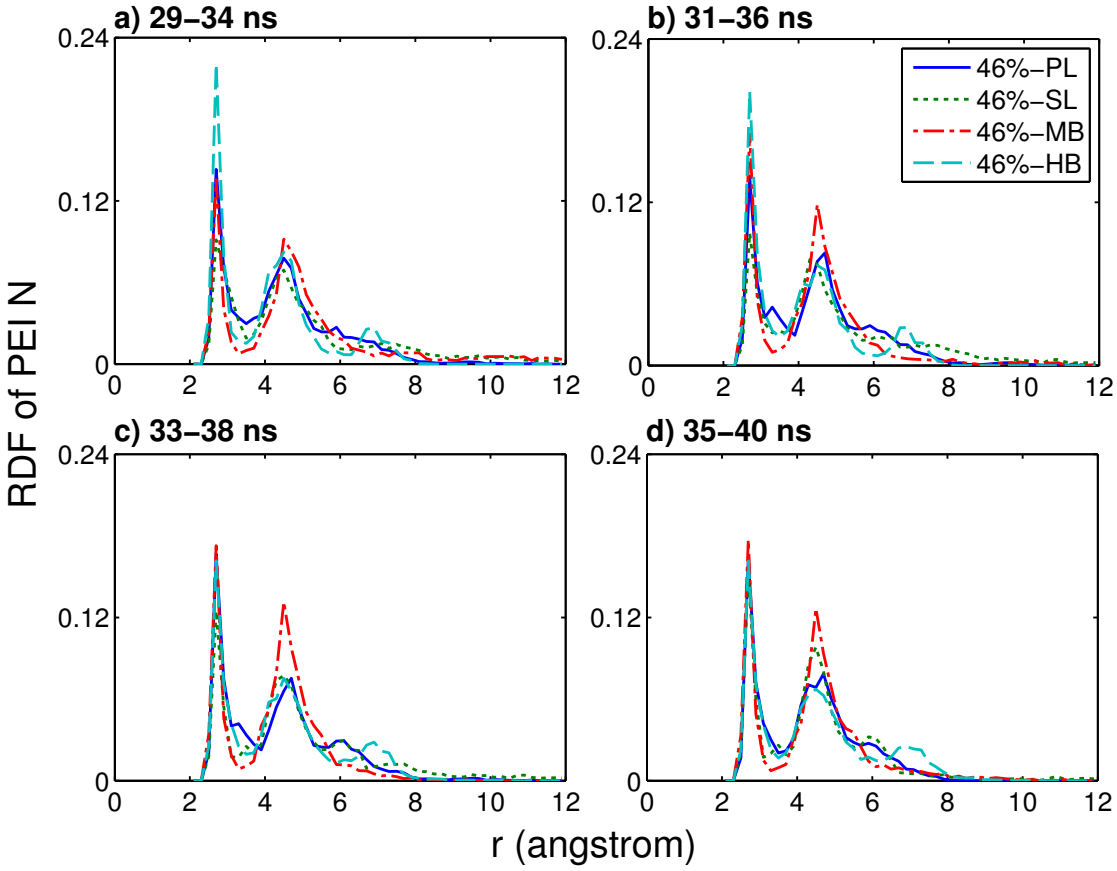

Figure S28: Radial distribution functions of all PEI nitrogens around the DNA backbone oxygens for the 46% systems, plotted for different simulation time windows. (a) 29–34 ns, (b) 31–36 ns, (c) 33–38 ns, (d) 35–40 ns.

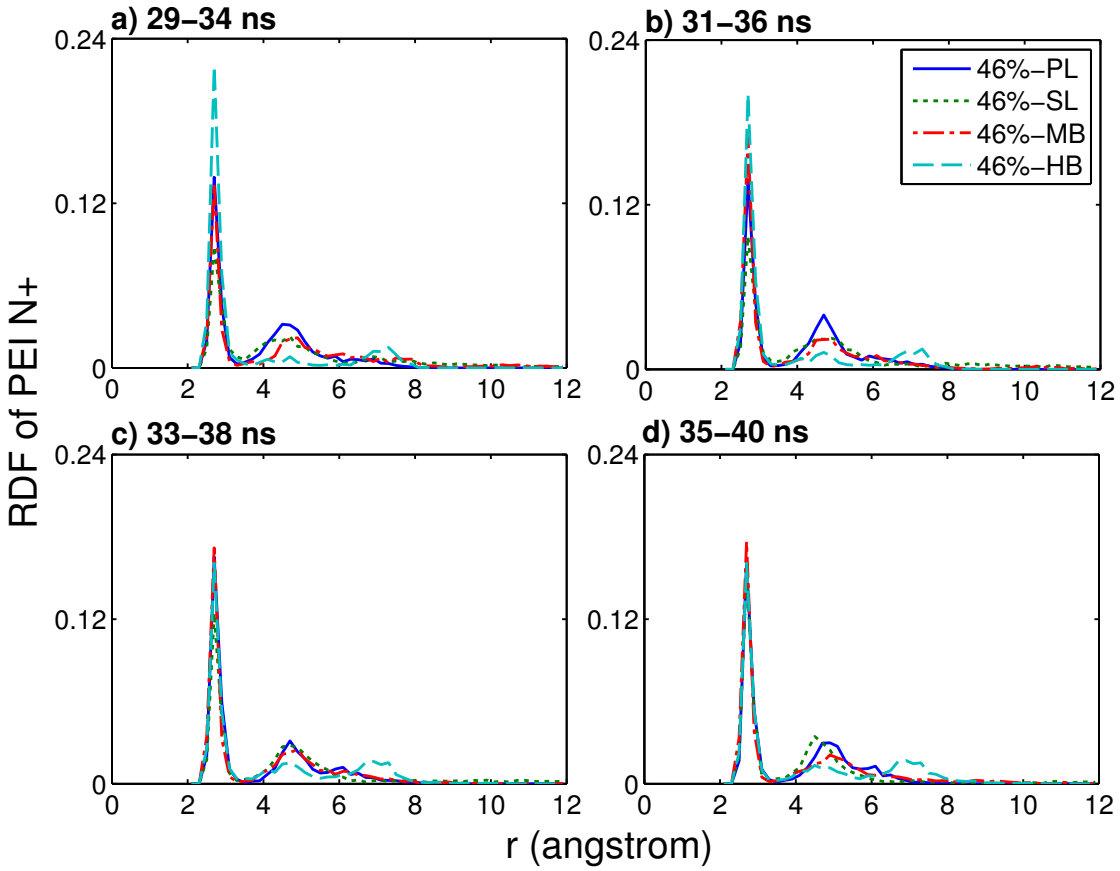

Figure S29: Radial distribution function of the PEI protonated nitrogens around the DNA backbone oxygens for the 46% systems, plotted for different simulation time windows. (a) 29–34 ns, (b) 31–36 ns, (c) 33–38 ns, (d) 35–40 ns.

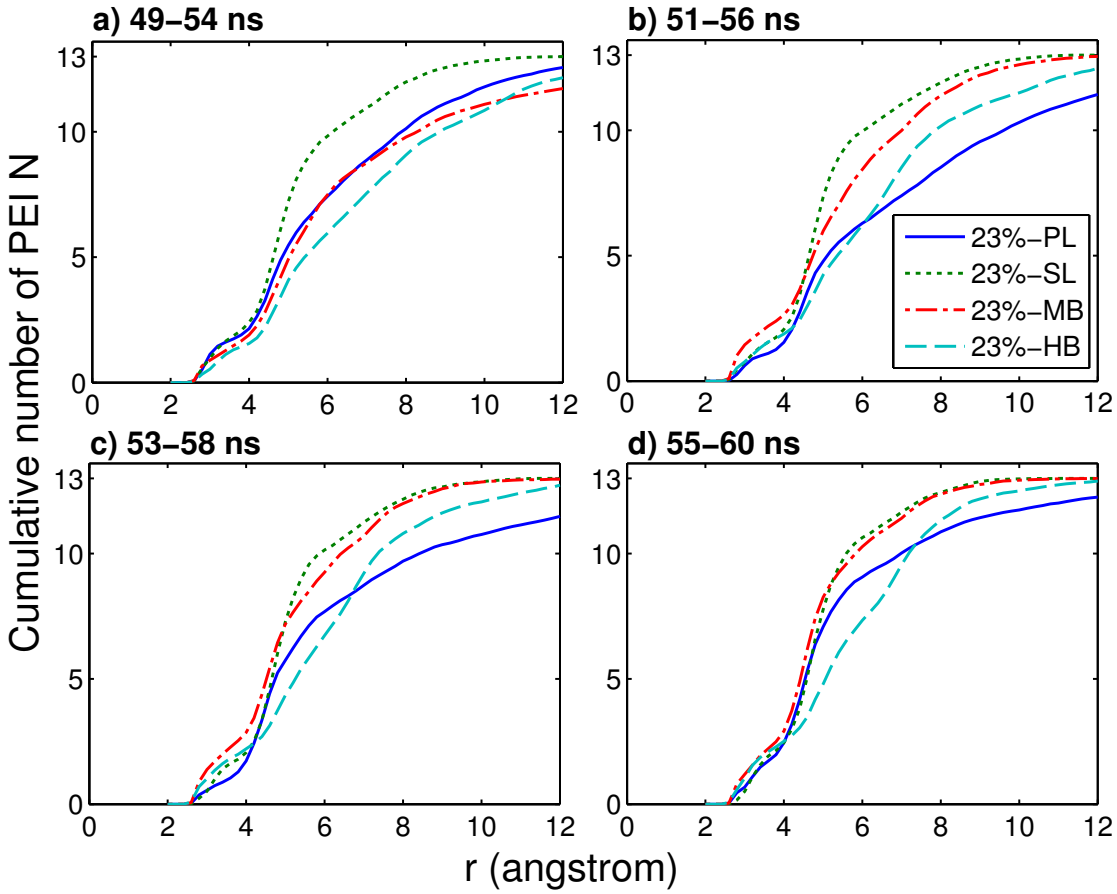

Figure S30: Cumulative number of the PEI nitrogens around the DNA backbone oxygens for the 23% systems, plotted for different simulation time windows. (a) 49–54 ns, (b) 51–56 ns, (c) 53–58 ns, (d) 55–60 ns.

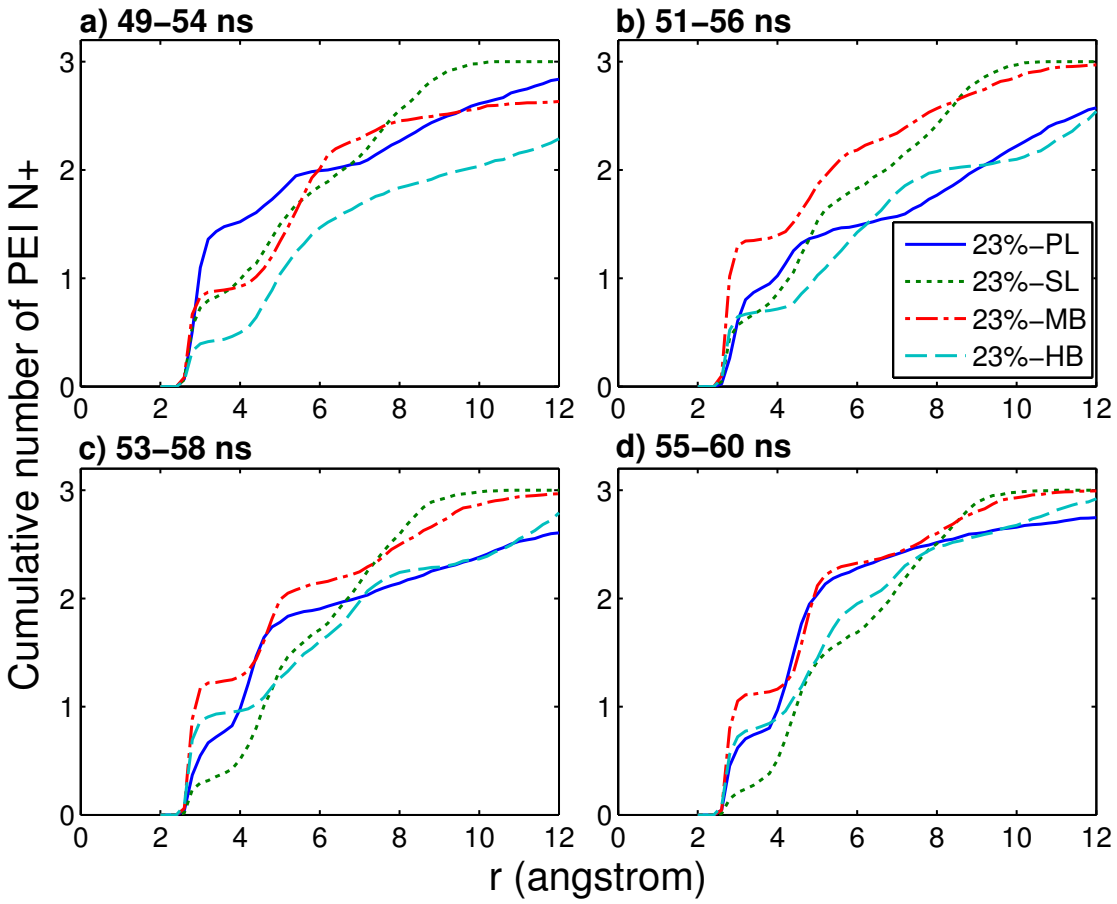

Figure S31: Cumulative number of the PEI protonated nitrogens around the DNA backbone oxygens for the 23% systems, plotted for different simulation time windows. (a) 49–54 ns, (b) 51–56 ns, (c) 53–58 ns, (d) 55–60 ns.

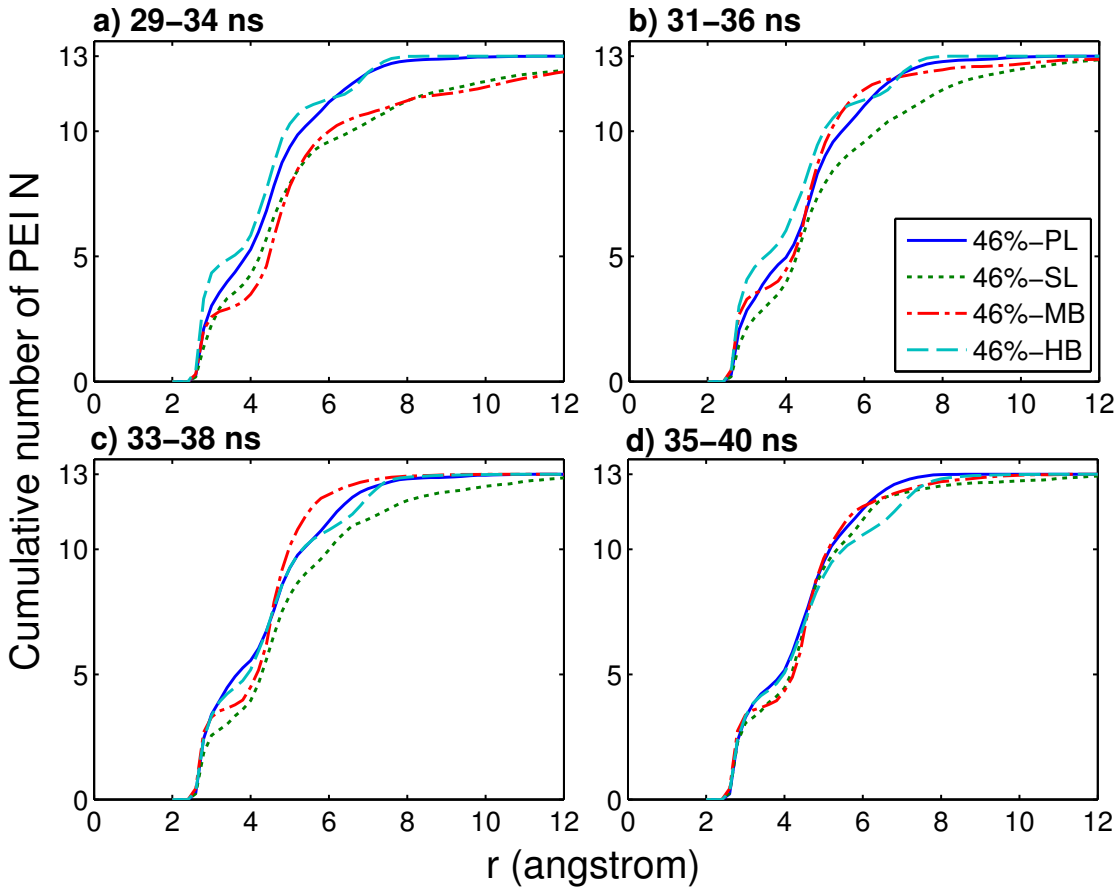

Figure S32: Cumulative number of the PEI nitrogens around the DNA backbone oxygens for the 46% systems, plotted for different simulation time windows. (a) 29–34 ns, (b) 31–36 ns, (c) 33–38 ns, (d) 35–40 ns.

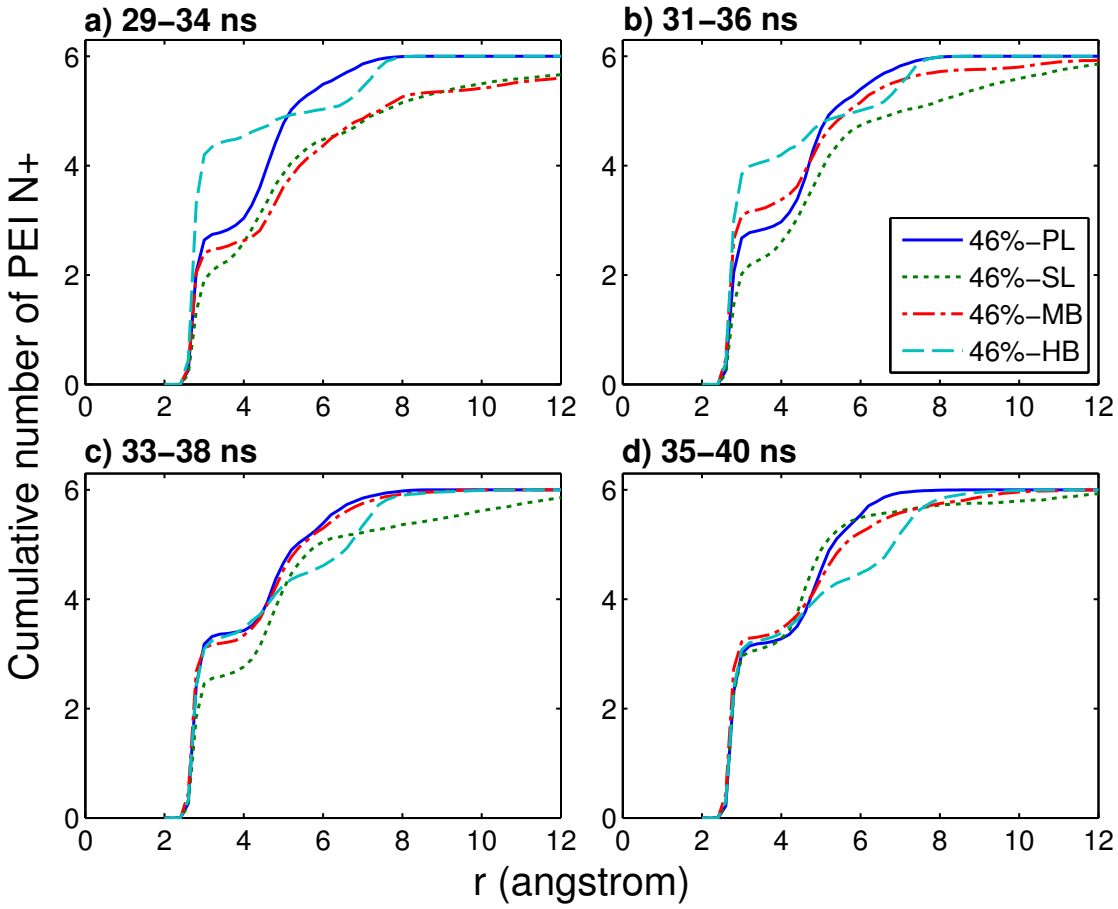

Figure S33: Cumulative number of the PEI protonated nitrogens around the DNA backbone oxygens for the 46% systems, plotted for different simulation time windows. (a) 29–34 ns, (b) 31–36 ns, (c) 33–38 ns, (d) 35–40 ns.

References

(1) Vanommeslaeghe, K.; Hatcher, E.; Acharya, C.; Kundu, S.; Zhong, S.; Shim, J.; Darian, E.; Guvench, O.; Lopes, P.; Vorobyov, I.; MacKerell, A. D., Jr. *J. Comput. Chem.* **2010**, *31*, 671–690.

(2) Ziebarth, J.; Wang, Y. *Biophys. J.* **2009**, *97*, 1971–1983.

(3) Reprinted from Biophysical Journal, Vol 97, Jesse Ziebarth and Yongmei Wang, Molecular Dynamics Simulations of DNA-Polycation Complex Formation, Pages No. 1971, Copyright (2009), with permission from Elsevier.

(4) Frisch, M. J. et al. *Gaussian 09 Revision A.1*, Gaussian Inc. Wallingford CT 2009.

(5) Brooks, B. R. et al. *J. Comput. Chem.* **2009**, *30*, 1545–1614.

(6) Dong, H.; Hyun, J.; Durham, C.; Wheeler, R. *Polymer* **2001**, *42*, 7809–7817.